

---

# Neural Likelihoods via Cumulative Distribution Functions

---

Pawel Chilinski

Department of Statistical Science University College London

Ricardo Silva

## Abstract

We leverage neural networks as universal approximators of monotonic functions to build a parameterization of conditional cumulative distribution functions. By a modification of backpropagation as applied both to parameters and outputs, we show that we are able to build black box density estimators which are competitive against recently proposed models, while avoiding assumptions concerning the base distribution in a mixture model. That is, it makes no use of parametric models as building blocks. This approach removes some undesirable degrees of freedom on the design on neural networks for flexible conditional density estimation, while implementation can be easily accomplished by standard algorithms readily available in popular neural network toolboxes.

## 1 CONTRIBUTION

We show how to parameterize conditional cumulative distribution functions (CDFs) for continuous data using neural networks. We explain how training can be done by a simple adaptation of standard neural network learning methods. The motivation is supervised learning problems where the regression framework is not adequate. That is, problems where the representation of the output distribution as signal and noise leads to bad fit due to heteroscedastic multimodality and skewness in the conditional distribution. We also discuss multivariate extensions, required for multi-output supervised learning and for unsupervised learning.

Bishop (1994) discusses examples where modeling the full distribution of the output variable in a supervised learning problem is more sensible than a typical re-

gression formulation. This lead to variations for unsupervised learning (e.g., Uria et al., 2013), among other developments. Common to many of these methods is the reliance on mixture models: neural networks (or other functional representations) encode the mean, variances and mixture probabilities of a predetermined set of Gaussians, or the equivalence parameters of other (conditional) mixture models.

Our method has the following main conceptual advantages: (i) we bypass any mixture model construction, which not only requires a choice of number of mixture components, but also a choice of base distribution. This is not an obvious choice. See the discussion by Uria et al. (2013), which proposes variations of mixture models with Gaussians and Laplace distributions to be decided empirically. Common to these is the reliance on a parametric building block; (ii) we work on the space of CDFs, in which the required constraints are comparatively easy when contrasted to density functions and which can be tackled by simple modifications of standard programming tools. For instance, the method by Murray et al. (2009) constructs unnormalized densities nonparametrically, which requires a sophisticated algorithmic machinery of local moves to sidestep the normalization problem.

At the same time, we do not claim we have no shortcomings. The methods here described are not optimized for high-dimensional density estimation, where parameter sharing helps but which we treat as an orthogonal and out of scope issue. The cost of calculating the likelihood is admittedly higher than in a mixture model, but only by a constant factor in the case of univariate and some multivariate variations. Our neural network CDFs have several attractive computational properties, including exact likelihood and tail area evaluation, but sampling from them in general requires numerical function inversion methods. Ultimately, we do not defend that any universal method for flexible conditional density estimation, a very hard problem, will be a clear winner in all practical tasks. We do defend that more general methods that require no parametric component on top of a neural network structure provide a conceptual advancement of general interest to the community.

This paper is organized as follows. In Section 2 we describe our main approach. Related work, including that on neural network methods for density estimation and monotonic function representations, is described in Section 3. Experiments are discussed in Section 4. From an empirical analysis perspective, we focus on density estimation in order to keep the focus on a particular training criterion, but estimation of quantiles, tail area probabilities and outlier detection are other natural possibilities we leave for future work.

## 2 THE MONOTONIC NEURAL DENSITY ESTIMATOR

In this section, we introduce the Monotonic Neural Density Estimator (MONDE), inspired by neural network methods for parameterizing monotonic functions. Description of related work is postponed to Section 3. The primary usage of MONDE is to model conditional densities as encoded from conditional CDFs. Unconditional joint distributions follow as a special case. We start with the simplest but important univariate case, where dependency between variables does not have to be modelled. We progress through more complex constructions to conclude with the most complex case, where we deal with multivariate data without assuming any specific families of distributions for the data generating process.

Here we use the following notation.

$F(\mathbf{y}|\mathbf{x})$ : Multivariate Conditional Distribution,  $\mathbf{y} \in \mathbb{R}^K$  is the response vector and  $\mathbf{x} \in \mathbb{R}^D$  is a covariate vector (which can be empty).

$F_k(y_k|\mathbf{x})$ : Marginal Conditional Distribution.

$f(\mathbf{y}|\mathbf{x})$ : Multivariate Conditional Probability Density Function (pdf).

$f_k(y_k|\mathbf{x})$ : Marginal Conditional Density

$w$ : the set of parameters of a neural network, with  $w_{ij}^l$  representing a particular weight connecting two nodes  $i$  and  $j$ , with  $i$  located at layer  $l$  of the network.

### 2.1 Univariate Case

MONDE for univariate responses is presented in Figure 1 as a directed acyclic graph (DAG) with two types of edges and a layered structure so that two consecutive layers are fully connected, with no further edges. The definition of layer in this case follows immediately from the topological ordering of the DAG. Covariates  $x_1, \dots, x_D$  and response variable  $y$  are nodes without parents in the DAG, with the layer of the covariates defined to be layer 1. Response variable  $y$  is positioned in some layer  $1 < l_y < L$ , where  $L$  is the final layer. Each

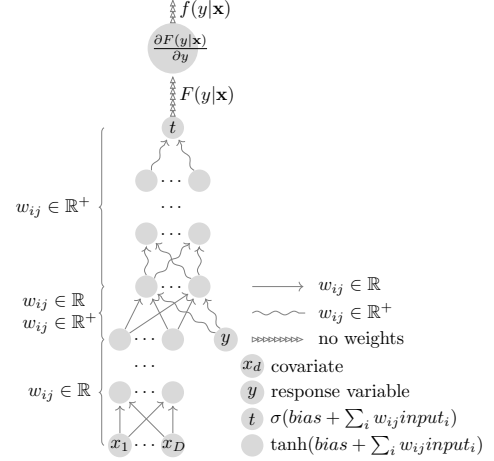


Figure 1: The Univariate Monotonic Neural Density Estimator architecture, MONDE.

intermediate node  $i$  at layer  $l$ ,  $h_i^l$ , returns a non-linear transformation of a weighted sum of all nodes in layer  $l-1$ . For concrete purposes, here we use the hyperbolic tangent function,  $h_i^l = \tanh\left(\sum_{v_j \in \mathcal{V}_{l-1}} w_{ij}^l v_j + w_{i0}^l\right)$ , where  $1 < l < L$  and  $\mathcal{V}_l$  is the set of nodes in layer  $l$ . The final layer  $L$  consists of a single node  $t(y, \mathbf{x}) \equiv \text{sigmoid}\left(\sum_{v_j \in \mathcal{V}_{L-1}} w_{ij}^L v_j + w_{i0}^L\right)$ , representing the probability  $P(Y \leq y | \mathbf{X} = \mathbf{x})$  as encoded by the weights of the neural net. In other words,  $t(y, \mathbf{x})$  is interpreted as a CDF  $F_w(y | \mathbf{x})$  encoded by some  $w$ .

Assuming  $w$  generates a valid CDF, we can use an automatic differentiation method to generate the density function  $f_w(y | \mathbf{x})$  corresponding to  $F_w(y | \mathbf{x})$  by differentiating  $t(y, \mathbf{x})$  with respect to  $y$ . The same principle behind backpropagation applies here, and in our implementation we used Tensorflow to construct the computation graph that generates  $t(y, \mathbf{x})$ . Once the pdf is constructed, automatic differentiation can once again be called, now with respect to  $w$ , in order to generate gradients that can be plugged into any gradient-based learning algorithm.

To guarantee that  $t(y, \mathbf{x})$  is a valid CDF, we must enforce three constraints: (i)  $\lim_{y \rightarrow -\infty} t(y, \mathbf{x}) = 0$ ; (ii)  $\lim_{y \rightarrow +\infty} t(y, \mathbf{x}) = 1$ ; (iii)  $\partial t(y, \mathbf{x}) / \partial y \geq 0$ . A sufficient condition to accomplish this is as follows: for every  $w_{ij}^l$  where  $v_j \in \mathcal{V}_{l-1}$  is a descendant of  $y$  in the corresponding DAG, enforce  $w_{ij}^l \geq 0$ . This means that for all layers  $l > l_y$ , all weights  $\{w_{ij}^l\}$  are constrained to be non-negative, while  $\{w_{i0}^l\}$  are unconstrained. Meanwhile,  $w_{ij}^l \in \mathbb{R}$  for  $l \leq l_y$ . In Figure 1, the constrained weights are represented as squiggled edges. This guarantees monotonicity condition (iii). Due to the range of the logistic function being on  $[0, 1]$ , (i) and (ii) are also guaranteed. See Section 3 for further discussions.

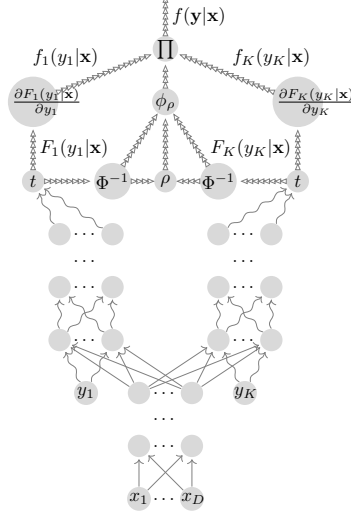


Figure 2: Multivariate Monotonic Neural Density Estimator with Gaussian Copula Dependency and Constant Covariance

## 2.2 Multivariate Gaussian Copula Models

A standard way of extending univariate models to multivariate models is to use a copula model (Sklar, 1959; Schmidt, 2006). In a nutshell, we can write a multivariate CDF  $F(\mathbf{y})$  as  $F(\mathbf{y}) = P(\mathbf{Y} \leq \mathbf{y}) = P(F^{-1}(F(\mathbf{y})) \leq \mathbf{y}) = P(\mathbf{U} \leq F(\mathbf{y}))$ . Here,  $\mathbf{U}$  is a random vector with uniformly distributed marginals in the unit hypercube and  $F^{-1}(\cdot)$  is the inverse CDF, which will be unique for continuous data as targeted in this paper. The induced multivariate distribution with uniform marginals,  $P(\mathbf{U} \leq \mathbf{u})$ , is called the *copula* of  $F(\cdot)$ . Elidan (2013) presents an overview of copulas from a machine learning perspective.

This leads to a way of creating new distributions. Starting from a multivariate distribution, we extract its copula. We then replace its uniform marginals with any marginals of interest, forming a *copula model*. In the case of the multivariate Gaussian distribution, the density function

$$f(y_1, \dots, y_K) =$$

$$\phi_\rho(\Phi^{-1}(F_1(y_1)), \dots, \Phi^{-1}(F_K(y_K)))f_1(y_1)\dots f_K(y_K)$$

is a Gaussian copula model where  $\phi_\rho$  is a Gaussian density function with zero mean and correlation matrix  $\rho$ ,  $\Phi^{-1}$  is the inverse CDF of the standard Gaussian, and  $f_k(\cdot)$  is any arbitrary univariate density function. We can show that the  $k$ -th marginal of this density is indeed  $f_k(\cdot)$ .

We enhance the density estimator from the previous section by exploiting two copula variations to handle a  $K$ -dimensional multivariate output  $\mathbf{y}$ . The first variation is shown in Figure 2. Weight sharing is done so

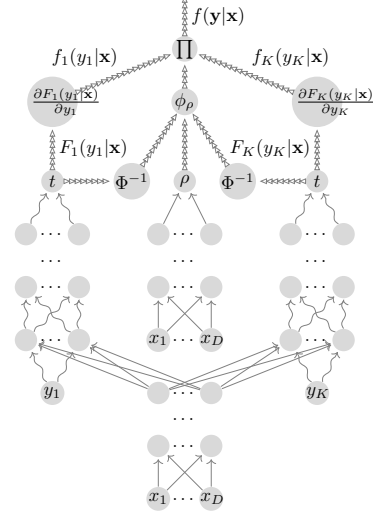


Figure 3: Multivariate Monotonic Neural Density Estimator with Gaussian Copula Dependency and Parameterized Covariance

that all output variables  $y_k$  are placed in layer  $l_y$ , with all weights  $w'_{ij}$ ,  $l' \leq l_y$ , producing transformations of the input  $\mathbf{x}$  that is shared by all conditional marginals  $F_k(y_k | \mathbf{x})$ . From layers  $l_y + 1, \dots, L$ , the neural network is divided in  $K$  blocks with no overlap, generating  $K$  outputs  $t_k(y_k, \mathbf{x})$ , each representing an estimate of the corresponding marginal  $F_k(y_k | \mathbf{x})$ . They can be jointly trained by maximizing the marginal composite likelihood (Varin et al., 2011)  $\prod_k \partial t_k(y_k, \mathbf{x}) / \partial y_k$  in mini-batches of data points (that is, each marginal pdf can be obtained by again applying backpropagation with respect to each  $y_k$ ).

Once fitted by marginal composite likelihood, the individual marginal distributions evaluated at each training point are transformed via standard normal quantile functions. Such quantiles  $\Phi^{-1}(F_k(y_k | \mathbf{x}))$  are marginally standard normal variables, which we use to estimate the correlation matrix for the entire training set. The estimated marginals and correlation matrix fully define our model. Taking product of the estimated copula and estimated marginal densities gives us an estimate of the joint density with a correlation matrix that does not change with  $\mathbf{x}$  but which is simple to estimate by re-using the univariate MONDE. We call this the Constant Covariance Copula Model.

The next improvement, achieved at a computational cost, consists of parameterizing the correlation matrix using covariate transformations. The diagram of the model for bivariate distributions is presented in Figure 3. This time the correlation matrix is parameterized via a low rank factorization of the covariance matrix which is a function of the covariates, which allows to model data with heteroscedasticity in the copula of the

output variables. The correlation matrix parameterization is done as follows:

$$\mathbf{\Sigma}(\mathbf{x}) = \mathbf{u}(\mathbf{x}) \cdot \mathbf{u}(\mathbf{x})^T + \text{diag}(\mathbf{d}(\mathbf{x})) \equiv \quad (1)$$

$$\mathbf{D}(\mathbf{x}) \equiv \sqrt{\text{diag}(\mathbf{\Sigma}(\mathbf{x}))}, \quad (2)$$

$$\rho(\mathbf{x}) \equiv \mathbf{D}^{-1}(\mathbf{x}) \cdot \mathbf{\Sigma}(\mathbf{x}) \cdot \mathbf{D}^{-1}(\mathbf{x}), \quad (3)$$

where  $\mathbf{\Sigma}(\mathbf{x})$  is the covariate parameterized low rank covariance matrix;  $\mathbf{u}(\mathbf{x}) \in \mathbb{R}^K$  and  $\mathbf{d}(\mathbf{x}) \in \mathbb{R}_+^K$  are covariate parameterized vectors; *diag* is an operator which extracts a diagonal vector from the square matrix or creates diagonal matrix from a vector (according to context);  $\rho(\mathbf{x})$  is the resulting covariate parameterized correlation matrix. All of these parameters can be jointly updated by gradient-based methods.

### 2.3 Autoregressive Models

This variation of the MONDE model uses the same approach to univariate output distributions, which here is used to parameterize factors in a probabilistic DAG model: to capture dependence structure, we assume a given ordering  $y_1, \dots, y_K$ , defining the fully connected DAG model

$$f(\mathbf{y} \mid \mathbf{x}) = \prod_{k=1}^K f_k(y_k \mid \mathbf{x}, \mathbf{y}_{<k}), \quad (4)$$

where  $\mathbf{y}_{<k}$  is set of response variables with index smaller than  $k$ . In theory, the indexing of variables can be chosen arbitrarily. In this work, we do not try to optimize it. This type of DAG parameterization was called “autoregressive” in the neural density estimator of Uria et al. (2013), a nomenclature we use here to emphasize that this is a related method. However, in our contribution we remain agnostic about any sort of parameter sharing among factors, unlike the key feature of the work of Uria et al., which is best left to be tackled in future work.

### 2.4 PUMONDE: Pure Monotonic Neural Density Estimator

The last model presented in this paper is a multivariate conditional density estimator that uses higher order differentiation of the distribution function with respect to multiple response variables. The higher order derivative  $\partial t^K(\mathbf{y}, \mathbf{x}) / \partial y_1 \dots \partial y_K$  has to be non-negative so that the model can represent a valid density function. The graph representing a monotone function  $t_u(\mathbf{y}, \mathbf{x})$  with no finite upper bound (to be later “renormalized”) is presented in Figure 4. The output of this function is non-negative because the last transformation is softplus( $x \equiv \log(1 + \exp x)$ ). This function is non-decreasing with respect to any response variable on the same premises as previous

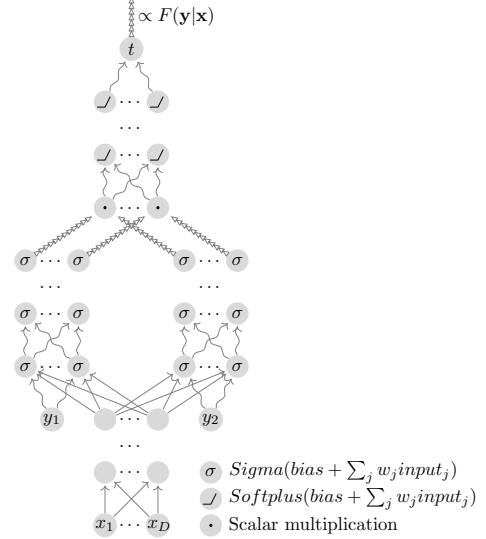


Figure 4: Graph of the “Unnormalized” Distribution Function of PUMONDE, Pure Monotonic Neural Density Estimator. This is illustrated for two target variables  $y_1$  and  $y_2$ , showing disjoint blocks of hidden units with sigmoid activation functions which at some point converge to hidden units with softplus activations.

marginal distributions. In this model, we replaced tanh with sigmoid and softplus, where a hidden unit uses softplus if it has more than one ancestor in  $y_1, \dots, y_K$ , sigmoid otherwise. This is because non-convex activation functions such as the sigmoid will not guarantee e.g.  $\partial^2 t(\mathbf{y}, \mathbf{x}) / \partial y_1 \partial y_2 \geq 0$  for units which have more than one target variable as an ancestor. Higher order derivatives with respect to the same response variable can take any real number because of properties of the computational graph i.e. using products of non-decreasing functions which are always positive and noting the fact that second order derivative with respect to the same response variable transformed by sigmoid can take any real value.

The density is then computed from the following transformations:

$$F_w(\mathbf{y} \mid \mathbf{x}) = \frac{t_u(\mathbf{y} \mid \mathbf{x})}{t_u(\mathbf{y}_{max} \mid \mathbf{x})}, \quad (5)$$

$$f_w(\mathbf{y} \mid \mathbf{x}) = \frac{\partial^K F_w(\mathbf{y} \mid \mathbf{x})}{\partial y_1 \dots \partial y_K}, \quad (6)$$

where  $\mathbf{y}_{max}$  is the vector containing maximum values of the response variables, which are assumed to be finite. In our empirical studies, this is estimated from the training data set. This normalization together with the guarantee of non-decreasing monotonicity and positiveness of the  $F_u$  with respect to each element of  $\mathbf{y}$  assures that the range of the distribution function is  $[0, 1]$  in the lower and upper limits of  $\mathbf{y}$ .

It must be stressed that an unstructured PUMONDE with full connections will in general require an exponential number of steps (as a function of  $K$ ) for the gradient to be computed, mirroring the problem of computing partition functions in undirected graphical models. Alternatives to be explored in the future include the use of composite likelihood (Varin et al., 2011) and its relationship to graphical models for CDFs (Huang and Frey, 2008; Silva et al., 2011). For now we will restrict PUMONDE to small dimensional problems.

### 3 RELATED WORK

In this section, we give an overview of the ideas that inspired our work and constitute the fundamental building blocks of our method.

#### 3.1 Monotonic Neural Networks for Function Approximation

The first approaches to constrain neural networks to monotonic functions of its inputs used penalty terms added to the cost function (Sill and Abu-Mostafa, 1996). No hard constraint is imposed, which for our purposes would mean negative density functions could still appear during training and test. Sill (1997) proposes a model that encodes a hard monotonicity constraint, which was deemed necessary to make learning efficient for regression functions obeying this property. The inputs are first transformed linearly to multiple groups by using constraint weights which are positive for increasing monotonicity and negative for decreasing monotonicity (weight constraints are enforced by exponentiating each free parameter). The groups are processed by a “max” operator and a “min” operator. The whole model can be learned by the gradient descent. The max operator models the convex part of the monotone function and the min operator models the concave part. Authors prove that their model can approximate any continuous monotone function with finite first partial derivative to a desired accuracy. This model has several hyper-parameters: number of groups or number of hyper-planes within the group. A variant of this work is introduced by Daniels and Velikova (2010).

Lang (2005) proves that if the output and hidden to hidden weights are positive for a single-layer network, then we can constrain input-to-hidden layers weights selectively to be positive/negative depending on monotonicity constraints on selected input variables. In this way, we can choose for which input variables we want to preserve monotonicity of the output. They also notice that min/max networks (Sill, 1997) tend to be more expensive to train than this simple neural net-

work architecture with constrained weights.

The review by Minin et al. (2010) test several approaches on variety of data sets which exhibit monotonicity on some of the inputs. Authors conclude that there is no definite winner and evaluated approaches excel in different areas and applications.

#### 3.2 Neural Density Estimation

One of the first methods to build conditional density estimators using neural networks was the Mixture Density Networks (MDNs) of Bishop (1994). The main motivation behind this work is the inability of standard regression models to summarize multimodal outputs with conditional means. MDNs parameterize conditional mixtures of Gaussians where the neural network outputs mixing probabilities and Gaussian parameters for each mixture.

Another approach, presented by Wang (1994), trains a density estimator by fitting a monotonic neural network to match a smoothed empirical CDF. Unlike our work, this is solely a smoother that reconstructs the empirical CDF using a function approximator. There is no likelihood function nor supervised signal.

The method presented by Likas (2001) tackles the problem of normalizing the output of a neural network to directly approximate density functions. It uses numerical integration over the domain of the function.

Two methods are presented by Magdon-Ismael and Atiya (2002) for unconditional density estimation using neural networks and CDFs. They both rely on the empirical CDF as targets to be approximated, with no explicit likelihood function being used at any moment during training. The reliance on the empirical CDF to provide training signal also implies that there is no straightforward way of adapting it to the conditional density estimation problem.

Zegers and Johnson (2006) compare different approaches to construct objective to be optimized when building neural density estimators: KL-divergence, MC approximation and maximum entropy. They also propose an empirical approach to check consistency of the model.

The approach based on the autoregressive factorized representation of the density function is presented by Larochelle and Murray (2011) and Uria et al. (2013). In the continuous case, the proposed model parameterizes each conditional marginal using what is essentially a MDN (Bishop, 1994). All neural networks that parameterize the mixtures partially share parameters, in a way that also speeds up computation as the number of parameters grows linearly with dimensionality. The model is extended in Uria et al. (2014) to use deep

neural network to parameterize ensemble of factorial orderings of directed representation.

Trentin (2016) notices that using a neural network to approximate the CDF function, and then differentiating it to obtain a density function estimate, can give poor results. This does not affect MONDE, as our objective function maximizes the likelihood function instead of directly approximating a measure of distance to the empirical CDF as done by, e.g., Magdon-Ismail and Atiya (2002). His proposal includes a model of the density function that must be normalized numerically.

Zhang (2018) improves on the work of Magdon-Ismail and Atiya (2002), which comes from using hard monotonicity constraints instead of the penalization approach used by the other authors.

## 4 EXPERIMENTS

In this section, we describe experiments performed and method used to compare models on various data sets. We split each data set into train, validation and test partitions. Models are only trained on the train partition. Hyperparameters are chosen based on the log likelihood computed on the validation set. We use Scikit-Optimize library to do hyperparameters search. It uses Gaussian process-based optimization to estimate a function of model likelihood with respect to hyperparameters. We found it performs better than ordinary random grid search. We also do early stopping using validation set to prevent overfitting. The best model on the validation set is chosen and log-likelihoods of test points are computed. We compare the models performance by running pair wise t-test on these values.

Models developed in this paper are compared to the following baseline models: RNADE with Gaussian and Laplace mixtures (Uria et al., 2013), deep orderless RNADE with Gaussian and Laplace mixtures (Uria et al., 2014) and Mixture Density Networks with Gaussian mixtures (Bishop, 1994).

We set up the datasets in a way to test model performance when we need to approximate density functions for conditional, unconditional, univariate and multivariate cases. To achieve this we arrange the data sets with different dimensionality of response vector and covariate vector. Dimensions of all data sets are given in Table 1.

### 4.1 Synthetic Data

Results from experiments with the synthetic data are shown in Table 2. We draw univariate Gaussian and Student-t data with means parameterized by a sinu-

data set	observations	x dimension	y dimension
sin normal	10000	1	1
sin t	10000	1	1
inv sin normal	10000	1	1
inv sin t	10000	1	1
uci redwine 2d	1599	7	2
uci redwine unsupervised	1599	0	9
uci whitewine 2d	4898	1	2
uci parkinsons 2d	5875	13	2
mv nonlinear	10000	1	2
uci whitewine unsupervised	4898	0	3
uci parkinsons unsupervised	5875	0	15
etf 1d	1073	1	1
etf 2d	1073	2	2
FX all assets predicted	28781	16	8
FX EUR and GBP predicted	28773	32	2
FX EUR predicted	28749	80	1

Table 1: Dimensions and sizes of data sets.

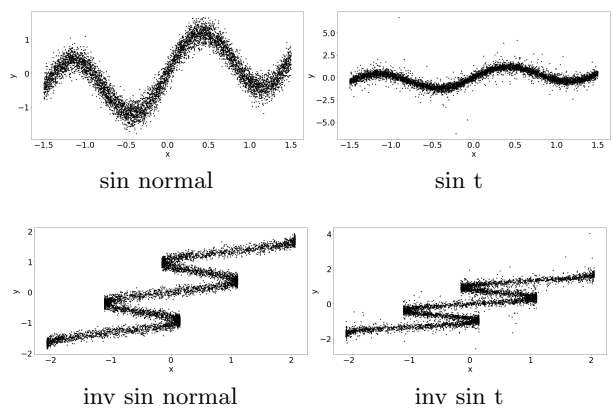


Figure 5: Samples from the generated univariate data.

soid shape having a positive linear trend with respect to the covariate. We also test the models by inverting the data so we can check whether they can capture the multimodality of the response. Additionally, we generate data from the bivariate Gaussian distribution where the mean of each response variable is parameterized by a different nonlinear function with respect to the covariate. The response variables in this case are correlated and have different variances. We show the datasets in Figure 5 and 6.

Fitting the data by conditional mean models, such as a regular neural network with mean squared error, is not suitable in the case when we deal with multimodality. In this case, we should be using models that find the probabilistic structure in the data. We show in Figure 7 that proposed and baseline models can capture it.

In Figure 8, we show density heatmaps of the marginal  $f(y_0, y_1 = 0 | x)$  from the bivariate distribution that generated the data, baseline and proposed models. We see that RNADE and MDN models have problems encoding the probabilistic structure, but our models can capture it well, which is also confirmed by the test log-likelihood evaluations shown in Table 2.

	RNADE Laplace	RNADE Normal	RNADE Deep Normal	RNADE Deep Laplace	MONDE Const Cov	MONDE Param Cov	MONDE AR	PUMONDE	MDN Const Cov	MDN Param Cov	True LL
data set											
sin normal	0.115	0.118	<b>0.155</b>	0.130	0.136				0.134		0.176
sin t	-0.200	-0.193	<b>-0.194</b>	-0.205	<b>-0.178</b>				-0.317		-0.163
inv sin normal	0.186	0.212	<b>0.253</b>	0.226	0.174				0.227		
inv sin t	-0.083	-0.109	-0.132	<b>-0.063</b>	-0.089				-0.199		
mv nonlinear	-6.196	-6.067	-5.695	-5.281	-5.095	-5.074	-5.135	<b>-5.033</b>	-5.247	-5.702	-4.973

Table 2: Generated data mean loglikelihoods on test partition.

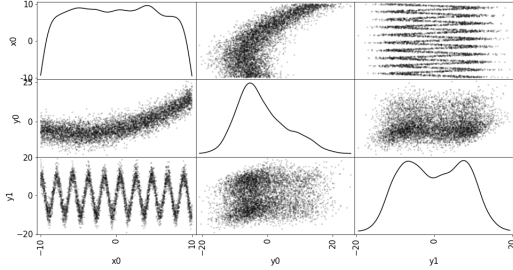


Figure 6: Samples from the generated multivariate data. Panels in the diagonal show marginal pdfs.

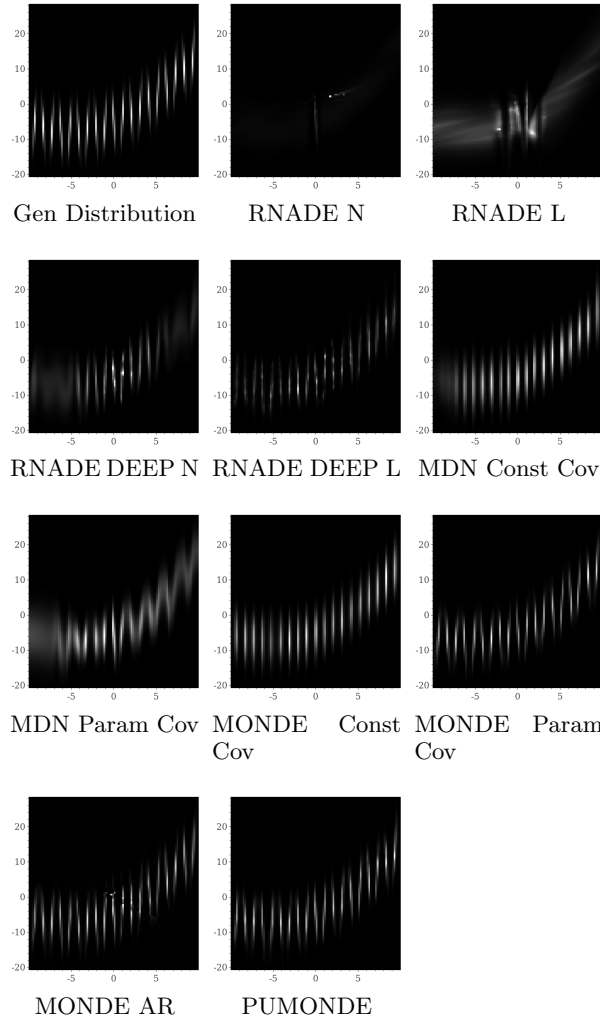


Figure 8: Nonlinear bivariate marginal  $f(y_0, y_1 = 0 | x)$  density heatmap.

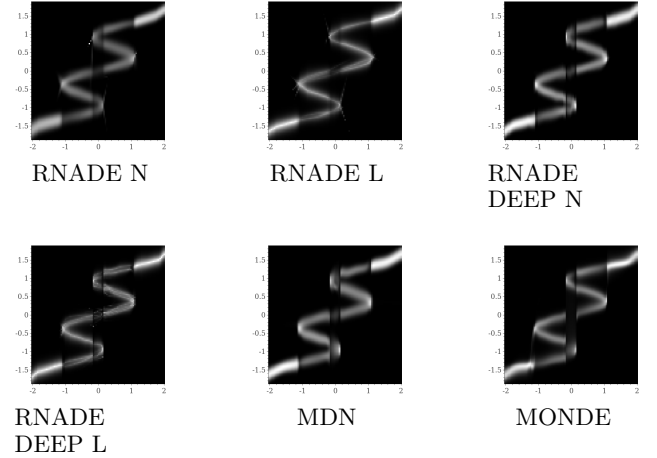


Figure 7: Density heatmap computed from the models for the inverse sinusoid normal noise data set.

## 4.2 Low Dimensional Data

The results from the experiments with UCI datasets (Dheeru and Karra Taniskidou, 2017) are shown in Table 3. The UCI datasets are preprocessed in the same way as done by Uria et al. (2013) i.e., we removed categorical variables and variables which have absolute value of Pearson coefficient correlation with other variable larger than 0.98. We use each UCI dataset in two separate experiments. First, by setting the two last columns as response variables (ordering as defined by the documentation of the data), while the remaining columns constitutes the covariates. Those are the datasets with suffix “2d” in our discussion. Second, by using all columns as response variables, hence assuming the covariates vector to be empty. Those datasets are given the suffix “unsupervised.”

We see that not assuming any parametric family of distributions can bring considerable improvements on out of sample performance of the model. Additionally, we report that when we trained models in datasets where some columns have a considerably small number of unique values (but still deemed as real values by the dataset documentation), the RNADE models tend to “overfit” by placing very narrow Gaussians at partic-

	RNADE Laplace	RNADE Normal	RNADE Deep Normal	RNADE Deep Laplace	MONDE Const Cov	MONDE Param Cov	MONDE AR	PUMONDE	MDN Const Cov	MDN Param Cov
data set										
uci redwine 2d	-2.543	-2.506	-3.310	-2.343	-2.672	-2.462	<b>-1.795</b>	<b>-1.997</b>	-2.269	-2.250
uci redwine unsupervised	-6.574	-6.496	-8.244	-8.297	-2.992	<b>-1.879</b>	-8.077		-8.676	-9.314
uci whitewine 2d	-1.958	-1.956	-1.957	-1.968	-1.910	<b>-1.891</b>	<b>-1.915</b>	<b>-1.901</b>	-1.961	-1.940
uci parkinsons 2d	-1.406	-1.323	-1.424	-2.910	-4.032	-4.766	<b>-1.134</b>	-1.254	-1.368	-2.425
uci parkinsons unsupervised	0.999	0.304	-3.265	-3.214	1.328	-3.654	<b>3.055</b>		-0.870	-3.798

Table 3: UCI data sets mean loglikelihoods on test data.

	RNADE Laplace	RNADE Normal	RNADE Deep Normal	RNADE Deep Laplace	MONDE Const Cov	MONDE Param Cov	MONDE AR	PUMONDE	MDN Const Cov	MDN Param Cov
data set										
etf 1d	<b>-1.416</b>	-1.495	<b>-1.422</b>	<b>-1.408</b>	<b>-1.383</b>				<b>-1.398</b>	
etf 2d	-1.501	<b>-1.472</b>	-1.857	-1.588	<b>-1.426</b>	<b>-1.466</b>	<b>-1.401</b>	-1.599	<b>-1.441</b>	-1.634
FX EUR predicted	<b>-1.054</b>	-1.074	-1.093	-1.272	-1.081				-1.185	
FX EUR GBP predicted	-2.070	-2.072	-2.268	<b>-2.024</b>	-2.292	-2.162	-2.074	-2.048	-2.130	-2.307
FX ALL predicted	-2.940	-2.985	-3.479	-3.741	-4.853	-8.107	<b>-2.838</b>		-5.604	-8.924

Table 4: Financial data sets mean loglikelihoods on test data.

ular points (the test likelihood is high, but this is an artifact of treating essentially discrete data as if had a density). Our models fitted smooth distributions. Only when we removed columns with few unique values we were able to train RNADE models to the satisfactory level of generalization. We set the threshold that if a given column has below 5% of unique values, compared to the number of samples, we remove it from the given data set.

### 4.3 Financial Data

The results from experiments with financial data sets are shown in Table 4. We use two different sources of the financial data.

First is the exchange traded funds downloaded from the Yahoo service. We obtain two time series of daily close prices between 03.01.2011 and 14.04.2015. The “etf 1d” are returns of the SPY symbol. The response and covariate variables in this data set are consecutive returns in the time series accordingly. The “etf 2d” are returns of the SPY and DIA symbols. The returns are aggregated into the final data set using the same transformation as in the fist univariate case, but this time both instrument returns are combined together so response and covariate vectors have two components.

Second is the foreign exchange tick data downloaded from FXCM repository<sup>1</sup>. We downloaded prices for the following currency pairs: EURUSD, GBPUSD, USDJPY, USDCHF, USDCAD, NZDUSD, NZDJPY, GBPJPY for the period between 05.01.2015 and 30.01.2015. Each currency pair dataset contains top of the book tick level bid and offer prices. We compute the returns of the mid point prices for these time

series. Then we subsample each time series using 1 minute interval and align all of them into one data frame. This table of all aligned currency pairs’ returns is used to create three data sets. “FX EUR predicted” contains the EURUSD return as the response variable and ten previous historical returns from all currency pairs as covariates i.e. if we have return for EURUSD at time  $t$  we gather for this response covariates as returns for all instruments at times  $t-1, t-2, \dots, t-10$ . “FX EUR and GBP predicted” is constructed as the previous one but with two response variables i.e. EUR and GBP returns and the covariates constructed from all four previous historical returns plus hour of day variable. “FX all assets predicted” contains all contemporaneous currency pairs returns as response and two autoregressive returns of all currency pairs as covariates. We see from the results table that there is improvement in using our approach in an autoregressive representation and other versions of our model can also be at par with recently proposed solutions.

## 5 Discussion

We proposed a new family methods for building likelihood functions with neural networks. For applications such as estimating tail area probabilities, one direction of work is learning about the uncertainty in our models, using for instance the ideas of Gal and Ghahramani (2016). More ambitiously, we want to continue this work as building blocks in more complex architectures, such as the neural models with the embedded memory like the Neural Turing Machine (Graves et al., 2014).

<sup>1</sup><https://github.com/fxcm/FXCMTickData>



---

## References

- Christopher M. Bishop. Mixture density networks. Technical report, Technical Report NCRG 4288, Neural Computing Research Group, Aston University, Birmingham, 1994.
- Benigno Uria, Iain Murray, and Hugo Larochelle. RNADE: the real-valued neural autoregressive density-estimator. In *Advances in Neural Information Processing Systems 26*, pages 2175–2183, 2013.
- Iain Murray, David MacKay, and Ryan P Adams. The Gaussian process density sampler. In *Advances in Neural Information Processing Systems 21*, pages 9–16, 2009.
- Abe Sklar. Fonctions de répartition à  $n$  dimensions et leurs marges. *Publications de l’Institut de Statistique de l’Université de Paris*, 8:229–231, 1959.
- T Schmidt. Coping with copulas. 2006.
- Gal Elidan. Copulas in machine learning. In *Copulae in Mathematical and Quantitative Finance*, pages 39–60. Springer, Berlin, 2013.
- Cristiano Varin, Nancy Reid, and David Firth. An overview of composite likelihood methods. *Statistica Sinica*, 21(1):5–42, 2011.
- Jim Huang and Brendan Frey. Cumulative distribution networks and the derivative-sum-product algorithm. *Proceedings of the 24th Conference on Uncertainty in Artificial Intelligence*, 2008.
- Ricardo Silva, Charles Blundell, and Yee Whye Teh. Mixed cumulative distribution networks. *AISTATS 2011*, pages 670–678, 2011.
- Joseph Sill and Yaser S. Abu-Mostafa. Monotonicity hints. In *Advances in Neural Information Processing Systems 9*, pages 634–640, 1996.
- Joseph Sill. Monotonic networks. In *Advances in Neural Information Processing Systems 10*, pages 661–667, 1997.
- Hennie Daniels and Marina Velikova. Monotone and partially monotone neural networks. *IEEE Trans. Neural Networks*, 21(6):906–917, 2010. doi: 10.1109/TNN.2010.2044803.
- Bernhard Lang. Monotonic multi-layer perceptron networks as universal approximators. In *Artificial Neural Networks: Formal Models and Their Applications - ICANN 2005, 15th International Conference, Warsaw, Poland, September 11-15, 2005, Proceedings, Part II*, pages 31–37, 2005. doi: 10.1007/11550907\6.
- Alexey Minin, Marina Velikova, Bernhard Lang, and Hennie Daniels. Comparison of universal approximators incorporating partial monotonicity by structure. *Neural Networks*, 23(4):471–475, 2010. doi: 10.1016/j.neunet.2009.09.002.
- Shouhong Wang. A neural network method of density estimation for univariate unimodal data. *Neural Computing and Applications*, 2(3):160–167, 1994. doi: 10.1007/BF01415012.
- Aristidis Likas. Probability density estimation using artificial neural networks. *Computer Physics Communications*, 135(2):167 – 175, 2001.
- Malik Magdon-Ismaïl and Amir F. Atiya. Density estimation and random variate generation using multilayer networks. *IEEE Trans. Neural Networks*, 13(3):497–520, 2002. doi: 10.1109/TNN.2002.1000120.
- Pablo Zegers and Jose G. Johnson. Consistent density function estimation with multilayer perceptrons. In *Proceedings of the International Joint Conference on Neural Networks, IJCNN 2006, part of the IEEE World Congress on Computational Intelligence, WCCI 2006, Vancouver, BC, Canada, 16-21 July 2006*, pages 1128–1135, 2006. doi: 10.1109/IJCNN.2006.246817.
- Hugo Larochelle and Iain Murray. The neural autoregressive distribution estimator. In *Proceedings of the Fourteenth International Conference on Artificial Intelligence and Statistics, AISTATS 2011, Fort Lauderdale, USA, April 11-13, 2011*, pages 29–37, 2011.
- Benigno Uria, Iain Murray, and Hugo Larochelle. A deep and tractable density estimator. In *Proceedings of the 31st International Conference on International Conference on Machine Learning - Volume 32, ICML’14*, pages I–467–I–475, 2014.
- Edmondo Trentin. Soft-constrained nonparametric density estimation with artificial neural networks. In *Artificial Neural Networks in Pattern Recognition - 7th IAPR TC3 Workshop, ANNPR 2016, Ulm, Germany, September 28-30, 2016, Proceedings*, pages 68–79, 2016. doi: 10.1007/978-3-319-46182-3\6.
- Shengdong Zhang. From CDF to PDF - A density estimation method for high dimensional data. *CoRR*, abs/1804.05316, 2018.
- Dua Dheeru and Efi Karra Taniskidou. UCI machine learning repository, 2017. URL <http://archive.ics.uci.edu/ml>.
- Yarin Gal and Zoubin Ghahramani. Dropout as a Bayesian approximation: Representing model uncertainty in deep learning. In *Proceedings of the 33rd International Conference on Machine Learning, ICML 2016, New York City, NY, USA, June 19-24, 2016*, pages 1050–1059, 2016.
- Alex Graves, Greg Wayne, and Ivo Danihelka. Neural Turing machines, 2014. cite arxiv:1410.5401.

# Neural Likelihoods via Cumulative Distribution Functions: Supplement

Pawel Chilinski

Department of Statistical Science University College London

Ricardo Silva

## 1 PUMONDE Considerations

In this section, we show why we chose the proposed computational graph for PUMONDE model. For simplicity of exposition, we focus on the bivariate case, but the explanation applies to the general multivariate case.

To obtain a valid distribution function  $F(y_1, y_2 | \mathbf{x})$  and the corresponding density function  $f(y_1, y_2 | \mathbf{x})$ , we need to constrain our neural network to meet following conditions:

1.  $\lim_{y_1 \rightarrow -\infty, y_2 \rightarrow -\infty} F(y_1, y_2 | x) = 0$
2.  $\lim_{y_1 \rightarrow +\infty, y_2 \rightarrow +\infty} F(y_1, y_2 | x) = 1$
3.  $\frac{\partial^2 F}{\partial y_1 \partial y_2} \in \mathbb{R}^+$
4.  $\frac{\partial^2 F}{\partial y_k^2} \in \mathbb{R}$  for  $k = 1, 2$

To meet constraints 1 and 2, we parameterize the distribution function as the ratio of non-negative monotonic functions i.e.

$$F(y_1, y_2 | \mathbf{x}) := \frac{t(y_1, y_2, \mathbf{x}, \mathbf{w})}{t(y_{1 \max}, y_{2 \max}, \mathbf{x}, \mathbf{w})}.$$

We chose the end transform of  $t(y_1, y_2, \mathbf{x}, \mathbf{w})$  and all transforms that come after multiplication layer to be softplus (which will have symbol  $s_+$  here) function, first because it meets the requirement for the output to be non-negative and monotonically increasing with respect to its inputs. We also used  $s_+$  and not, for example,  $\tanh$ , because the simultaneous derivative of  $s_+$  with respect to  $y_1$  and  $y_2$  derivative is positive (the softplus function is convex in all of its domain). The  $\tanh$  derivative with respect to  $\{y_1, y_2\}$  can be negative, which it would break constraint 3. The multiplication layer in the middle of the computational graph, which receives positive valued transformations of  $y_1$  and  $y_2$  (because transformed by the sigmoid,  $\sigma$ ), allows us to fulfill constraint 3. This comes from the

fact that

$$\frac{\partial^2 s_+(\sigma(g_1(y_1)) \times \sigma(g_2(y_2)))}{\partial y_1 \partial y_2} = \quad (1)$$

$$\frac{\partial s'_+(\cdot) \times \sigma(g_1(y_1)) \times \sigma'(g_2(y_2)) \times g'_2(y_2)}{\partial y_1} = \quad (2)$$

$$\partial s''_+(\cdot) \times \sigma(g_2(y_2)) \times \sigma'(g_1(y_1)) \times g'_1(y_1) \times \sigma'(g_2(y_2)) \times g'_2(y_2) \quad (3)$$

where  $g_1$  and  $g_2$  are monotonic transformations of  $y_1$  and  $y_2$  using sigmoids, where the derivative with respect to the input is positive. The  $s'_+(\cdot)$  notation is used to show computation of the derivative of the function with respect to its input from the previous expression.

Therefore, that last expression always evaluates to a non-negative number. We see that, if we used *sigmoid* or *tanh* in the layers following the multiplication layer, we would not be guaranteed to obtain a non-negative result. Using the sigmoid activation function before the multiplication layer still allows to meet constraint 4 because the second derivative of  $\sigma$  with respect to its input can be positive and negative (because function is convex and concave depending on the input). It is also imperative that the input into the multiplication layer of PUMONDE is non-negative, because otherwise it would break the monotonic property of the model with respect to response variables.

## 2 Implementation Considerations

We found that the implementation of models using mixture components like RNADE and MDN requires a few tricks to make them work. First, we needed to tweak the minimum value allowed for the scale parameters of the Gaussian components. If we allow it to be arbitrarily small, the models frequently focused some of its mixture components on some points, which artificially inflated the average log likelihood. This is a well known problem with mixture models. We checked that to achieve the best performance of such models, the minimum value would have to be adjusted for each data set separately. In practice, we set this threshold to be the smallest one not causing the optimization

process to misbehave, taking into consideration the already large dimension of the hyperparameter space we optimize over.

### 3 Experiments Considerations

When we performed experiments using UCI datasets, we ran into difficulties when any particular column of data used as response variables contained few unique values. This happened even after taking into consideration fact that we removed all categorical variables beforehand, according to those which were marked as such in the dataset documentation. This was especially a problem for RNADE model, when one of such problematic variables was the first variable in the autoregressive expansion for the joint probability. In this case, because train, validation and test data contained a lot of points with the same values, RNADE could create overfitted first unconditional densities. This is not a realistic training procedure, since the data here is discrete for all practical purposes, resulting on unbounded test “densities” being easily achieved depending on the minimal scale allowed for a Gaussian mixture component in the training procedure. In Figure 1, we show an example of the  $f(y_1)$  density estimated by the RNADE model using a mixture of Laplace distributions, and the density of the same variable estimated by the autoregressive MONDE model. The data is the UCI whitewine dataset (used as an unsupervised case i.e. all variables treated as response variables with covariate set being empty). Our model was not influenced by these “continuous” variables with few unique values (compared to sample size), but to make the comparison more meaningful we removed columns with values which number of unique values constituted less than 5% of number of samples in the data set.

### 4 Source code

<https://github.com/pawelc/NeuralLikelihoods>

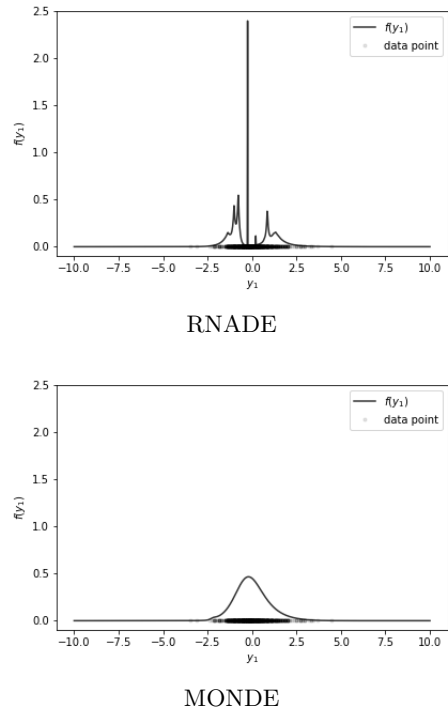


Figure 1: Densities estimated by the RNADE and MONDE AR models for the first variable in AR ordering when the corresponding variable had a small number of values. The data points are also shown on the  $x$  axis as black dots.